Available online at www.sciencedirect.com

ScienceDirect

Journal of Magnesium and Alloys 5 (2017) 35–40
www.elsevier.com/journals/journal-of-magnesium-and-alloys/2213-9567

Full Length Article

Microstructural evolution of die-cast and homogenized AZ91 Mg-alloys during dry sliding condition

Nagaraj M. Chelliah [a], Ram Kumar [a], Harpreet Singh [a,*], M.K. Surappa [b]

[a] Department of Mechanical Engineering, Indian Institute of Technology Ropar, Rupnagar, Punjab 140001, India
[b] Department of Materials Engineering, Indian Institute of Science, Bengaluru, Karnataka 560012, India

Received 16 July 2016; revised 24 January 2017; accepted 7 February 2017

Available online 22 February 2017

Abstract

Microstructural evolution of die-cast and homogenized AZ91 Mg-alloys was investigated during dry sliding wear condition. Tribological tests were performed using a pin-on-disc (EN8 steel) configuration with a normal load of 50 N at a constant sliding speed of 2.5 ms^{-1} under ambient environment. Delamination was recognized as a predominant wear mechanism in both of these materials. The die-cast AZ91 Mg-alloy exhibits lower coefficient of friction and higher wear rate. This can be ascribed to increase in the intensity of load bearing capacity of hard β-$Mg_{17}Al_{12}$ phase, and crack formation/de-cohesion at the interface between primary α-Mg and discontinuous β-$Mg_{17}Al_{12}$ phases. On the contrary, the homogenized AZ91 Mg-alloy experiences higher coefficient of friction and lower wear rate. The friction-induced microstructural evolution (supersaturated α-Mg to eutectic ($\alpha + \beta$-$Mg_{17}Al_{12}$)) tending to minimize the wear rate by providing barrier to material removal in the near surface region of homogenized AZ91 Mg-alloy. Therefore, experimental observation revealed that an inverse relationship exists between wear rate and coefficient of friction for the investigated materials. The analysis of worn surfaces and subsurfaces by electron microscopy provided evidence to delamination wear and microstructural evolution.

Keywords: Mg-alloys; Heat treatment; Microstructural evolution; Wear rate; Delamination; Subsurface

1. Introduction

Magnesium alloys have a significant potential in wide spectrum of engineering applications such as transport vehicles, electronics and bio-implant devices [1–3]. Despite the fact that AZ91 Mg-alloys show excellent casting properties and superior room temperature mechanical strengths, they are not suited for tribological applications [4–6] owing to brittle nature of β-$Mg_{17}Al_{12}$ intermetallic phase at the grain boundaries. Their tribological performance can be improved either by enhancing the level of ductility after dissolving β-$Mg_{17}Al_{12}$ phase through T4 solution heat treatment [7,8] or by reinforcing the matrix of AZ91 Mg-alloy with ceramic particles using metal matrix composite approach [9,10]. Aatthisugan et al. [9] showed that addition of both a hard reinforcement (e.g., B4C) and soft reinforcement (e.g., graphite) significantly improves the wear resistance of AZ91 Mg-alloy composites. Chen et al. [11] developed wear mechanism maps for AZ91 Mg-alloy by varying the sliding speed (0.1 to 2.0 ms^{-1}) and nominal load (1 to 350 N) under dry sliding condition. They indentified two main wear regimes namely mild wear and severe wear. While the mild wear regime had two sub wear-domains of oxidation and delamination wear, the severe wear regime comprised severe plastic deformation induced wear and melt induced wear. They also reported that transition in wear regime is predominantly controlled by frictional contact temperature.

Recently, Deepak et al. [12] investigated the effect of β-$Mg_{17}Al_{12}$ precipitates on the tribological behavior of AZ91 Mg-alloy. They reported that wear rate of age-hardened AZ91 Mg-alloy increased nearly by 10 times as compared to that of solution heat treated counterpart. Notice that they have performed all the tribological tests under mild wear regime. Moreover, they have not also considered the role of subsurface microstructural evolution on the dry sliding wear behavior of as-cast and heat treated AZ91 Mg-alloys.

Liang et al. [13] correlated the friction-induced microstructural evolution with wear behavior of AZ31 Mg-alloy. They noticed that dynamic recrystallization (DRX) within subsurface

* Corresponding author. Department of Mechanical Engineering, Indian Institute of Technology Ropar, Rupnagar, Punjab 140001, India. Fax: +91-1881-223395.
E-mail address: harpreetsingh@iitrpr.ac.in (H. Singh).

http://dx.doi.org/10.1016/j.jma.2017.02.001
2213-9567/

regime produces severe wear. They also developed an empirical model to predict the critical load for transition from mild into severe wear regime based on the kinetics of DRX process. Despite the fact that numerous studies are reported regarding dry sliding wear behavior of AZ91 Mg-alloys [14–17], influence of T4 heat treatment on dry sliding wear behavior of AZ91 Mg-alloy especially under severe operating condition (a normal load of 50 N and a sliding speed of 2.5 ms^{-1}) has not been reported yet to the best of our knowledge. Main objective of the present investigation is to establish the correlation between microstructural evolution and wear behavior of die-cast and homogenized AZ91 Mg-alloys under a dry sliding contact through detailed subsurface analysis.

2. Experimental methods

2.1. Heat treatment

The chemical composition of die-cast AZ91 Mg-alloy is given in Table 1. The specimens were sectioned from the die-cast AZ91 Mg-alloy ingot, and machined to cylindrical pins; having a diameter of 6 mm and a length of 30 mm in order to perform tribological tests. Half of these pin specimens were subjected to T4 solution heat treatment to modify their as-cast microstructural characteristics. Heat treatment of the die-cast AZ91C Mg-alloy was performed at a temperature of 425 °C under Argon environment for the period of 48 hours in order to minimize the tendency of oxidation or burning related issues with magnesium pins. These die-cast and homogenized specimens were designated as dc-AZ91 and ht-AZ91, respectively.

2.2. Pin-on-disc tests

A tribometer (CETR UMT, DFH-100, USA) was utilized to perform the dry sliding wear tests on both dc-AZ91 and ht-AZ91 pin specimens using pin-on-disk configuration. EN8 steel was used as the counter-face disk (with a diameter of 70 mm and a thickness of 5 mm). The specimens were properly cleaned with ethanol solution using an ultrasonicator for 10 min before the tribological tests. The tribological tests were performed at a constant sliding speed of 2.5 ms^{-1} and a normal load of 50 N for a sliding distance of 1500 m under ambient environment. The worn-out pins were weighed before and after each test run using single-pan electronic balance (a resolution of 0.1 mg). Wear debris were also collected after each test run for wear debris analysis. Wear rate for the tested specimens was quantified based on the difference in volumetric losses per unit sliding distance before and after the sliding tests. Friction force and normal force were continuously recorded by a load cell in order to evaluate coefficient of friction (COF) during sliding contact. Each of the tests was repeated three times to ensure repeatability in the friction and wear data, such that each reported value of COF and wear rate is an average of three observations.

2.3. Material characterization

Microstructures of the as-cast and heat treated composite specimens were analyzed by an optical microscope (Leica DM2700, Germany). Microstructures, worn-out surfaces, subsurface regimes, and wear debris morphologies of the investigated specimens were characterized by a scanning electron microscope (JEOL JSM-6610LV, Japan). Diffraction spectra were obtained to indentify various phases in as-cast/heat treated composite specimens and wear debris particles using an X-Ray Diffractometer (PANalytical X'pert-Pro (MPD), Netherlands). Micro-hardness tester (Wilson Instrument, Model 401/402 MVD, UK) was used to evaluate Vickers micro-hardness of the investigated specimens at a load of 100 gf for a dwell time of 15 seconds. Fracture toughness of the composite specimens was also estimated in three point bending mode by Tinius Olsen universal testing machine in accordance with the procedure mentioned in Ref. [7].

3. Results and discussion

3.1. Effect of heat treatment on microstructures

Fig. 1(a)–(b) depict the difference in microstructures of as-cast and heat treated AZ91 Mg-alloy. The dc-AZ91 specimen consists of two phases, namely primary α-Mg/eutectic (α + β) phase, and discontinuous precipitates of β-$Mg_{17}Al_{12}$ phase, which are distributed at the vicinity of grain boundaries. On the other hand, ht-AZ91 specimen comprised mainly single phase supersaturated α-Mg along with few traces of residual β-$Mg_{17}Al_{12}$ phase at the grain boundaries. The area fraction of β-$Mg_{17}Al_{12}$ phase in dc-AZ91 and ht-AZ91 was estimated to be around 24.3 ± 5% and 5.14 ± 2 %, respectively. It is well-known fact that solution T4 heat treatment leads to the dissolution of discontinuous precipitates of β-$Mg_{17}Al_{12}$ phase into the primary phase of α-Mg matrix [18]. This is the main reason behind reduction in the area fraction of β-$Mg_{17}Al_{12}$ phase in ht-AZ91 specimen as compared to that of ac-AZ91 specimen.

3.2. Frictional behavior

Bowdon and Tabor model [19] predicted that friction force is composed of two physical components namely, ploughing and adhesion. While ploughing component arises from the degree of plastic deformation in the contacting surfaces, adhesion component emerges from adhesive force existing between the contacting surfaces. Fig. 2(a) and 2(b) show SEM micrographs of worn surfaces for the dc-AZ91 and ht-Az91 specimen, respectively. The presence of grooves on the worn surfaces indicates that ploughing component controls the frictional

Table 1
Typical chemical composition of as-received die-cast Mg-alloy.

Mg-alloy	Chemical composition (wt%)						
AZ91C	Al	Zn	Mn	Si	Fe	Cu	Ni	Mg
	8.3–9.7	0.3–1.0	0.15–5.0	0.1 Max	0.005 Max	0.03	0.002	Balance

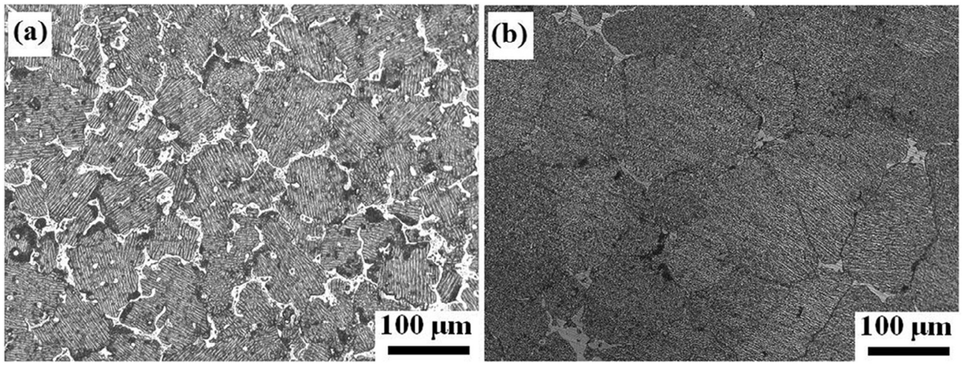

Fig. 1. Optical micrographs of the investigated specimen (a) die-cast AZ91 Mg-alloy and (b) heat treated AZ91 Mg-alloy at 425 °C for 48 h.

behavior rather than the adhesive component of friction. The width of grooves formed on the worn surfaces has increased for the ht-AZ91 specimen as compared to that of dc-AZ91 specimen (compare Fig. 2(a) Fig. 2 (b)). In addition, the wavy nature of deformed layers formed on the worn surface is also a clear signature of the increased plastic deformation for ht-AZ91 specimen as depicted in Fig. 2(d). As observed in Table 2, friction data revealed that the ht-AZ91 exhibits a higher coefficient of friction as compared to that of dc-AZ91 specimen. When AZ91 Mg-alloy is subjected to solution heat treatment, there occurs a significant reduction in the intensity of brittle and hard β-$Mg_{17}Al_{12}$ phase as mentioned earlier. This led to increase the level of ductility which aids in enhancing the ploughing component of friction by assisting significant plastic deformation on the worn surface. For the case of dc-AZ91 specimen, the presence of hard β-$Mg_{17}Al_{12}$ phase leads to increase the load bearing capacity which eventually resulted in lower coefficient of friction.

3.3. Correlation between microstructural evolution and wear behavior

According to delamination theory of wear [20], when shear force induced by sliding contact exceeds the interfacial shear strength between the secondary phase and the matrix material, de-cohesion occurs in the subsurface region leading to produce the thin and long wear debris of the contacting surfaces. As shown in Fig. 2(c) plate-like features along with crater patterns on the worn surfaces provide evidence for the existence of delamination wear mechanism. As summarized in Table 2, it can be seen that the wear rate of ht-AZ91 is significantly reduced by about 85% as compared to that of dc-AZ91 specimen. Deepak et al. [12] mentioned that age-hardened AZ91

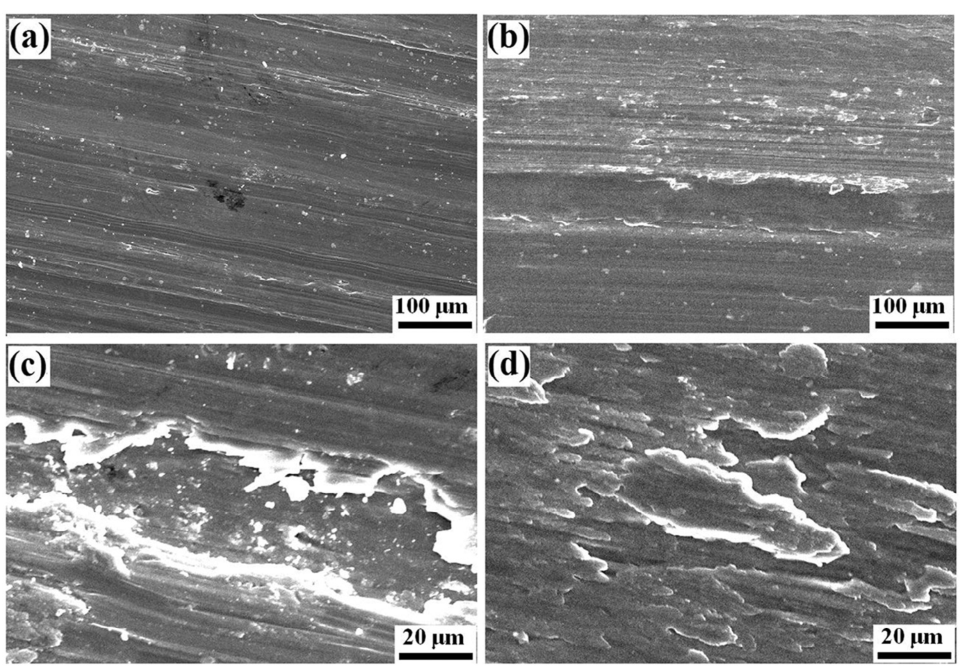

Fig. 2. Worn surfaces of the investigated specimen slid at 2.5 ms^{-1} with normal load of 50 N. (a) and (c) die-cast AZ91 Mg-alloy: (b) and (d) heat treated Az91 Mg-alloy.

Table 2
Summary of collected data from the present investigation.

Properties	dc-AZ91 Mg-alloy	ht-AZ91 Mg-alloy	Percentage change %
Microhardness (HV0.1)	76.57 ± 3.5	63.21 ± 4.2	−17.5%
Fracture toughness MPa.m$^{1/2}$	9.30 ± 1.7	12.62 ±	+35.7%
Coefficient of friction	0.10 ± 0.03	0.22 ± 0.04	+120%
Wear rate × 10^{-10} (m^3/m)	11.5 ± 1.6	1.87 ± 0.4	−83.791%

exhibits higher wear rate as compared to that of homogenized AZ91 due to the existence of brittle β-$Mg_{17}Al_{12}$ phase. They justified that higher amount of β-$Mg_{17}Al_{12}$ precipitates in age-hardened specimen reduce the real area of contact and subsequent increment in the localized contact pressure leading to increase the wear rate. The level of ductility and fracture toughness are believed to be enhanced in the case of ht-AZ91 specimen owing to the dissolution of brittle β-$Mg_{17}Al_{12}$ phase. Therefore, ht-AZ91 specimen experiences lower wear rate during dry sliding condition. Friedrich et al. [21] mentioned that wear rate of composite materials inversely scales with fracture toughness. Notice that the measured fracture toughness of ht-AZ91 is found to be greater than that of ac-AZ91 specimen (Table 2).

Liang et al. [13] pointed out that friction induced subsurface microstructure greatly influences the wear rate of AZ31 Mg-alloy. In order to establish a correlation between microstructural evolution and wear behavior, a detailed analysis of subsurface zones was conducted. Fig. 3(a) and Fig. 3(b) clearly depict the presence of large amount of β-$Mg_{17}Al_{12}$ phase in the subsurface zone for dc-AZ91 specimen, whereas there exists only a meager amount of β-$Mg_{17}Al_{12}$ phase in the ht-AZ91 specimen. It is interesting to investigate the role of friction-induced microstructural evolution on the wear behavior of ht-AZ91 specimen. The maximum friction temperature experienced by ht-AZ91 specimen was estimated to be about 421 °C in accordance with numerical model proposed by Zhang et al. [22]. This friction temperature is almost equivalent to the eutectic temperature (420 °C) for the AZ91 Mg-alloy [23]. Therefore, the supersaturated α-Mg phase can be transformed into stable eutectic (α + β) phase during sliding contact. This in-situ eutectic reaction within the subsurface region is given by the following equation [23]:

$$Supersaturated\ \alpha: Mg \rightarrow Primary\ \alpha: Mg + \beta: Mg_{17}Al_{12} \qquad (1)$$

The existence of alternating layers of α-Mg and β-$Mg_{17}Al_{12}$ phases as shown in Fig. 3(d) confirms the in-situ formation of eutectic phase during sliding contact. Under typical wear condition, the ductile α-Mg phase experiences significant plastic deformation before it is sheared away by fracture in the near surface region of ht-AZ91 specimen leading to minimize the wear rate for ht-AZ91 specimen. On the contrary, the presence of brittle β-$Mg_{17}Al_{12}$ phase in the subsurface zone of dc-AZ91 specimen (Fig. 3(c)) was subjected to intense crack formation within primary α-Mg phase, and de-cohesion especially at the interface between primary α-Mg and β-phase. This led to increase in the wear rate for the dc-AZ91 specimen.

SEM micrographs of the collected wear debris during dry sliding contact are illustrated in Fig. 4(a) through 4(d). It can be seen that wear debris of dc-AZ91 specimen were brittle in nature, whereas debris of ht-AZ91 specimen showed wavy pattern demonstrating ductile characteristics. The analysis of single wear debris of ac-AZ91 specimen exhibited cleavage fracture pattern, whereas ht-specimen represents river-like pattern along with evidence of detached subsurface layers merging one over the other as observed in Fig. 4(c) and Fig. 4(d).

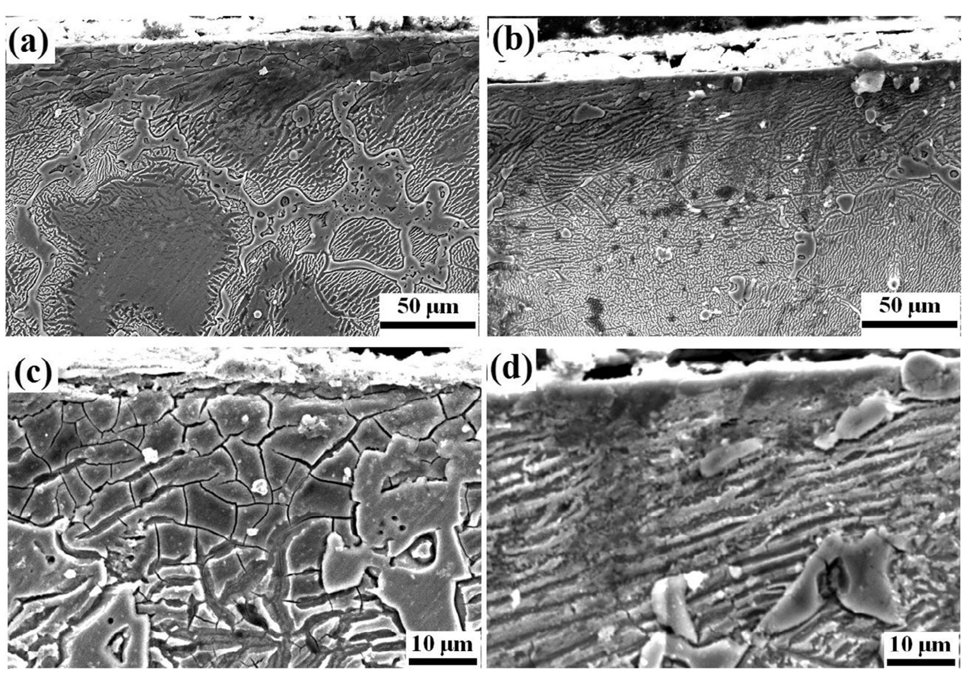

Fig. 3. Subsurface zone of the investigated specimen slid at 2.5 ms^{-1} with normal load of 50 N. (a) and (c) die-cast AZ91 Mg-alloy: (b) and (d) heat treated Az91 Mg-alloy.

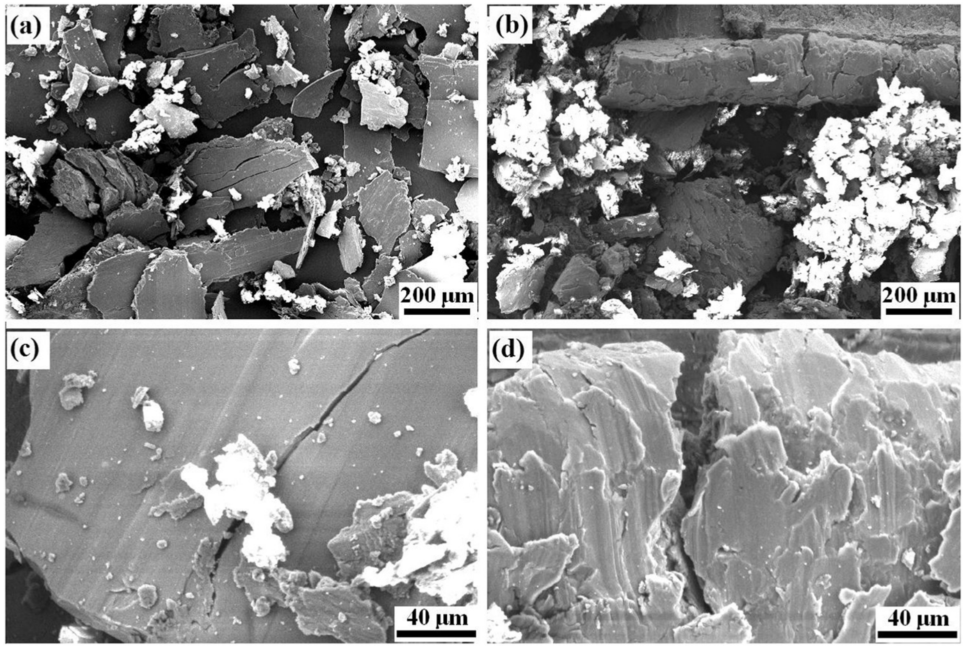

Fig. 4. Wear debris particles of the investigated specimen slid at 2.5 ms^{-1} with normal load of 50 N. (a) and (c) die-cast AZ91 Mg-alloy: (b) and (d) heat treated Az91 Mg-alloy.

Fig. 5 shows the XRD spectra of the collected wear debris particles in dc-AZ91 and ht-AZ91 specimen. It can be seen that dominant textures in the collected wear debris changed from pyramidal (1 0 - 1 1) into basal (0 0 0 2) in the case of dc-AZ91 and ht-AZ91 specimens, respectively. In other words, ht-AZ91 specimen exhibits higher peak intensity of basal plane at value of 2-theta at about 34.5 as compared to non-basal slip planes (prismatic and pyramidal) which are centered at 2-theta values of about 32.5 and 36.5. This change in crystallographic texture occurs due to variation in the intensity of plastic deformation at different crystallographic planes between ht-AZ91 and dc-AZ91 specimen. A stronger basal intensity in ht-specimen implies that it underwent plastic deformation along the basal plane and produced lower wear rate during sliding contact. Such trend in basal plane alignment appears to be contradictory with data reported by Takaomi et al. [24]. For instance, they indicated that formation of basal-plane alignment on the wear surfaces negatively affects the wear-resistance properties of AZ91 Mg-alloy. They mentioned that wear tends to progress easily due to the shear stress by friction when slip deformation occurs along the Mg basal plane at a low critical resolved shear stress (CRSS). However, ht-AZ91 specimen experiences better wear resistance even after it shows strong basal intensity. The reason behind such contradictory observation in the present work can be explained as follows. As seen in Fig. 3(b), subsurface microstructure comprised in-situ formed eutectic phases of α-Mg and β-$Mg_{17}Al_{12}$ in the subsurface region of ht-AZ91 specimen. Although the sliding wear becomes easier for α-Mg phase due to the alignment of basal plane as suggested by Takaomi et al. [24], subsequent β-$Mg_{17}Al_{12}$ phase in the near surface region provides significant barrier to material removal owing to its superior hardness [25]. This means that the secondary phase which slows down the rate of material removal, i.e. β-$Mg_{17}Al_{12}$ phase, controls the wear rate of ht-AZ91 Mg-alloy. On the contrary, there is no such in-situ formed eutectic phase in the subsurface region of dc-AZ91 specimen. Furthermore, the presence of discontinuous β-$Mg_{17}Al_{12}$ phase precipitates at the vicinity of grain boundaries may induce severe intergranular fracture in the subsurface region tending to increase the wear rate of dc-AZ91 Mg-alloy.

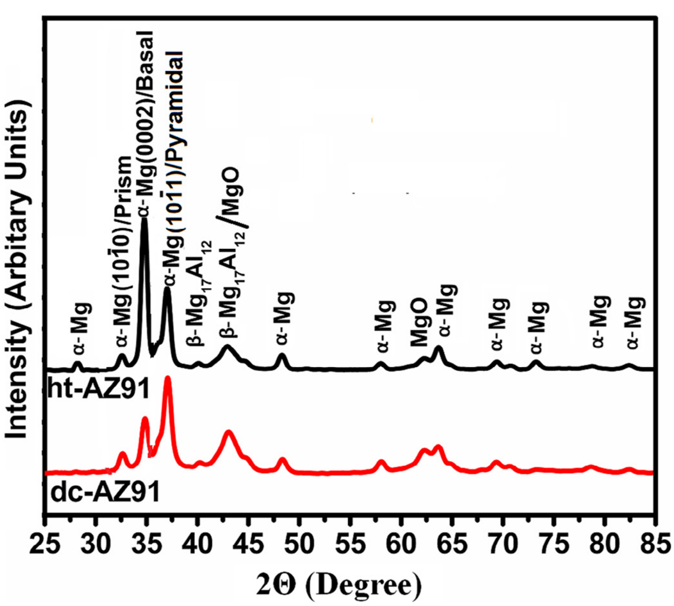

Fig. 5. XRD spectra of the collected wear debris particles slid at 2.5 ms^{-1} with normal load of 50 N.

In summary, experimental observation indicated that there exists an inverse relationship between coefficient of friction and wear rate for the investigated AZ91 Mg-alloys. This type of inverse trend is also observed by Mathew et al. [26] during dry sliding contact of MoS_2 coatings performed on Al-alloy substrates. Furthermore, T4 heat treatment is found to be advantageous to AZ91 Mg-alloy with regard to enhance its wear resistance.

4. Conclusions

1. Under chosen operating condition, dry sliding wear behavior of die-cast and homogenized AZ91 Mg-alloys is governed by delamination wear mechanism and there exists inverse relationship between coefficient of friction and wear rate.
2. Coefficient of friction of homogenized AZ91 Mg-alloy is increased by 120% than that of as-cast AZ91 Mg-alloy. This can be ascribed to increase in the level of ductility owing to the dissolution of brittle β-$Mg_{17}Al_{12}$ phase. The lower coefficient of friction in die-cast AZ91 Mg-alloy is associated with load bearing capacity of hard β-$Mg_{17}Al_{12}$ phase.
3. Wear rate of homogenized AZ91 Mg-alloy is decreased by 6.21 times as compared to that of as-cast AZ91 Mg-alloy. The formation of in-situ eutectic phase ($\alpha + \beta$) leads to minimize the wear rate by providing significant barrier to material removal in the subsurface region. The higher wear rate in as-cast AZ91 is due to increase in the intensity of crack formation and de-cohesion owing to the presence of brittle β-$Mg_{17}Al_{12}$ phase in the subsurface region.

Acknowledgments

The authors would like to express their gratitude to Mr. Amit Kaushal, for his extensive help in XRD characterization.

References

[1] B.L. Mordike, T. Ebert, Mater. Sci. Eng. A 302 (2001) 37–45.
[2] E. Aghion, B. Bronfin, Mater. Sci. Forum 19 (2000) 350–351.
[3] H. Friedrich, S. Schumann, J. Mater. Proc. Tech. 117 (2001) 276–281.
[4] H. Hu, J. Mater. Sci. 33 (1998) 1579–1589.
[5] D.S. Mehta, S.H. Masoodand, W.Q. Song, J. Mater. Proc. Tech. 155 (2006) 919–932.
[6] P.J. Blau, M. Walukas, Tribol. Int. 33 (2000) 573–579.
[7] G.R. Ebrahimi, A. Maldar, R. Ebrahimi, A. Davoodi, Kovove Mater. 48 (2010) 277–284.
[8] L. Zheng, H. Nie, W. Liang, H. Wang, Y. Wang, J. Mag. Alloys 4 (2016) 115–122.
[9] I. Aatthusugan, A. Razal Rose, D. Selwyn Jebadurai, J. Mag. Alloys (2016) doi:10.1016/j.jma.2016.12.004.
[10] N.M. Chelliah, H. Singh, M.K. Surappa, J. Mag. Alloys 4 (2016) 306–313.
[11] H. Chen, A.T. Alpas, Wear 246 (2000) 106–116.
[12] D. Kumar, J. Jain, T. Bisht, A. Zindal, J. Tribol. 137 (2015) 021604.
[13] C. Liang, C. Li, X.X. Lv, J. An, Wear 312 (2014) 29–39.
[14] N.N. Aung, W. Zhou, L.E.N. Lim, Wear 265 (2008) 780–786.
[15] J. An, R.G. Li, Y. Lu, C.M. Chen, Y. Xu, X. Chen, et al., Wear 265 (2008) 97–104.
[16] A. Zafari, H.M. Ghasemi, R. Mahmudi, Wear 292–293 (2012) 33–40.
[17] S.Q. Wang, Z.R. Yang, Y.T. Zhao, M.X. Wei, Trib. Lett. 38 (2010) 39–45.
[18] G. Xu, L. Zhang, L. Liu, Y. Du, F. Zhang, K. Xu, et al., J. Mag. Alloys 4 (2016) 249–264.
[19] F.P. Bowden, D. Tabor, The Friction and Lubrication of Solids, Oxford University Press, Oxford, 1950.
[20] N.P. Suh, Wear 44 (1977) 1–16.
[21] K. Friedrich, Friction and Wear of Polymer Composites, Elsevier Science Publishers, Amsterdam, 1986, pp. 258–281.
[22] J. Zhang, A.T. Alpas, Acta Mater. 45 (1997) 513–528.
[23] T. Zhu, Z.W. Chen, W. Gao, J. Mater. Eng. Perform. 19 (2010) 860–867.
[24] T. Itoi, K. Gonda, M. Hirohashi, Wear 270 (2011) 606–612.
[25] M. Furui, Y. Ebata, H. Yamada, S. Ikeno, K. Sakikibara, S. Saikawa, Mater. Trans. 52 (2011) 285–291.
[26] M.A. Hamilton, L.A. Alvarez, N.A. Mauntler, N. Argibay, R. Colbert, D.L. Burris, et al., Trib. Lett. 32 (2008) 91–98.